In vitro study of human endothelial progenitor cells behaviour on nitrided Ni-free Ti-27Nb alloy

Raluca Ion, Yvan Bedouin, Thierry Gloriant, Gladiola Andruseac, Doina-Margareta Gordin, Anisoara Cimpean

Progress in Natural Science: Materials International 29 (2019) 466–471

HOSTED BY

ELSEVIER

Contents lists available at ScienceDirect

Progress in Natural Science: Materials International

journal homepage: www.elsevier.com/locate/pnsmi

Original Research

In vitro study of human endothelial progenitor cells behaviour on nitrided Ni-free Ti–27Nb alloy

Raluca Ion[a], Yvan Bédouin[b,c], Thierry Gloriant[b], Gladiola Andruseac[d], Doina-Margareta Gordin[b], Anisoara Cimpean[a,*]

[a] University of Bucharest, Department of Biochemistry and Molecular Biology, 91-95 Spl. Independentei, Bucharest, 050095, Romania
[b] Univ Rennes, INSA Rennes, CNRS, ISCR (Institut des Sciences Chimiques de Rennes), F-35000, Rennes, France
[c] CHU de Rennes, Pôle d'Odontologie et de Chirurgie Buccale, 35000, Rennes, France
[d] Department of Biomedical Science, Faculty of Medical Bioengineering, "Grigore T. Popa" University of Medicine and Pharmacy, Iasi, Romania

ARTICLE INFO

Keywords:
Titanium alloy
Nitriding
Endothelial progenitor cells
Biocompatibility
Inflammatory response

ABSTRACT

A superelastic Ni-free Ti–27Nb alloy has been synthesized and gas nitrided at high temperature to investigate its suitability for vascular implant applications. The cellular responses of human endothelial progenitor cells (EPCs) to both bare and nitrided Ti–27Nb alloy have been analyzed using Live/Dead staining, MTT assay, fluorescence microscopy and ELISA technique, as well as NiTi alloy for comparison. Live/Dead staining and MTT assay were performed to assess the cellular viability and proliferation, while fluorescence microscopy was used to analyze cell adhesion, cell morphology, and the expression of endothelial cell markers (VE-cadherin and von Willebrand factor). Secretion of the pro-inflammatory chemokine MCP (monocyte chemoattractant protein)-1 by the cells grown in contact with the analyzed materials was further verified using the enzyme-linked immunosorbent assay. The results obtained revealed that adhesion, spreading, viability, proliferation rate and phenotypic markers expression of EPCs were similar on the surfaces of Ti–27Nb and NiTi alloys. Cells exposed to nitrided Ti–27Nb surface exhibited significantly decreased inflammatory response, which may be beneficial for reducing in-stent restenosis incidence.

1. Introduction

The use of metallic stents is widely recognized as an effective treatment for occlusive vascular disease. Among the stent materials commercially available, NiTi alloy has been widely used due to its shape-memory or superelastic properties. However, the large concentration of nickel in the alloy remains a serious concern. It has been suggested that allergic reactions to nickel ions released from vascular stents might be one of the triggering mechanisms for the development of in-stent restenosis [1]. In addition, nickel ions have been shown to cause impairment of endothelial cells functions [2–6]. Thrombotic complications frequently occur when NiTi alloy is used for vascular implants in small arteries [7]. Therefore, great efforts are devoted to develop more biocompatible Ni-free shape memory and superelastic alloys aiming to eliminate the allergic and inflammatory effects caused by nickel ions.

Binary Ti–Nb alloys have attracted particular attention in the search for new Ni-free alloys due to their low stiffness and superelasticity related to the stress-induced martensitic transformation [8–10]. The interest in Ti–Nb alloys is further stimulated by the high biocompatibility of both Ti and Nb [11–13] and their increased resistance to corrosion in simulated body fluid [14]. Despite the benefits of the Ti–Nb binary alloys, few studies have explored their potential for biomedical applications [11,13,15,16] being mostly focused on dental and orthopedic applications. Thanks to its chemical composition and the applied thermomechanical treatment, a Ti–27Nb alloy composition (at. %) has been designed to present a martensitic transformation under stress that gives rise to a superelastic behaviour. The synthesis and the characterization of this alloy was the subject of previous works in which the superelastic behaviour of the Ti–27Nb alloy has been established [17,18]. Recently, a gas nitriding thermochemical treatment was applied to improve the surface properties of the alloy. This surface treatment significantly increases the alloy corrosion resistance in simulated body fluid as well as its superficial hardness [19] while preserving the bulk alloy superelastic property. Moreover, surface nitriding has also been reported to provide titanium alloys with better qualities in terms of cell proliferation, adhesion and function [20–26].

In the current study, we have conducted a parallel comparison of

* Corresponding author.
E-mail address: anisoara.cimpean@bio.unibuc.ro (A. Cimpean).

https://doi.org/10.1016/j.pnsc.2019.08.001
Received 18 February 2019; Received in revised form 25 July 2019; Accepted 4 August 2019
Available online 10 September 2019

the biological effects exhibited by bare/nitrided Ti–27Nb alloy, and the commercial NiTi stent material considered as a reference. Human endothelial progenitor cells (EPCs) were cultured both on NiTi and bare and nitrided Ti–27Nb alloy, and the effects of these materials on the cellular responses were examined, including cell morphology, viability, proliferation, functional markers expression and inflammation.

2. Materials and methods

2.1. Alloy synthesis and samples preparation

The Ti–27Nb (at %) alloy was synthesized by cold crucible levitation melting (CCLM, CELES induction furnace) under a pure Ar atmosphere. After solidification, the alloy was heat treated for 20 h at 850 °C to remove chemical segregation occurring during solidification. After that, the alloy was cold rolled up to 90% in thickness and disc samples were cut (13 mm diameter; 1 mm thickness) for the biological tests. All samples were solution treated at 850 °C for 0.5 h in the beta-phase field and water quenched to restore a fully recrystallized beta-microstructure from the cold rolled state in order to promote the superelastic behaviour of the alloy. The Ti–27Nb disc samples were mechanically polished first with silicon carbide abrasive papers (up to 4000 grit) and then with a felt disk containing finely abrasive silica powder (1 μm). Afterwards, they were ultrasonically cleaned in acetone, thoroughly washed with ethanol and dried in air. Part of the disc samples was superficially treated by gas nitriding. The treatment was carried out at 950 °C for 2 h under one controlled flow high purity nitrogen atmosphere in a conventional furnace with a silica tube. The NiTi samples used for comparison were provided by AMF Company (Lury-sur-Arnon, France) and they were mechanically polished in the same conditions.

2.2. Surface analysis methods

The surfaces of bare Ti–27Nb and nitrided Ti–27Nb alloys were characterized by X-ray diffraction (XRD, Panalytical, Cu_α radiation) to investigate the surface modification induced by the nitriding treatment. Bare Ti–27Nb, nitrided Ti–27Nb and NiTi disc samples were characterized by atomic force microscopy (AFM, CSM Instrument) in tapping mode with a silicon tip in order to evaluate the roughness of each sample type. 10 roughness values were obtained from 83 × 83 μm AFM scans taken in different areas of each analyzed surface. An average roughness value, R_a, was obtained (± standard deviation) for each surface.

2.3. Cell culture

Human EPCs, purchased from Amsbio, were maintained in EPC basal medium (cat. no. Z7030004) supplemented with human EPC growth medium supplements (cat. no. Z7030005) at 37 °C in 5% CO_2 atmosphere. Cells, received at passage 4, were used in this study at passages 5 and 6. In order to perform the planned experiments, EPCs were seeded onto the surfaces of materials at a density of 10^4 cells/cm^2 and maintained for up to 5 days in standard culture conditions. Prior to cell seeding, these samples were sterilized by soaking in 70 % ethanol for 30 min. The samples on each side were then rinsed twice for 30 min in sterile-filtered MilliQ water, air dried and exposed to ultraviolet light in a tissue culture hood, for 30 min.

2.4. Fluorescence labeling of actin cytoskeleton and vinculin

After 2 h and 24 h of culture, EPCs grown on metallic samples were fixed with 4% paraformaldehyde prepared in phosphate buffered saline (PBS), permeabilized and blocked with 0.1% Triton X-100/2% bovine serum albumin for 15 min and washed with PBS. The samples were then incubated with anti-vinculin antibody (Santa Cruz Biotechnology, dilution 1:50) for 2 h at room temperature, washed again with PBS and incubated for 1 h with Alexa Fluor 546-conjugated specific secondary antibody (Invitrogen, dilution 1:200). Afterwards, phalloidin conjugated with Fluorescein isothiocyanate (FITC) (10 μg/ml; Sigma-Aldrich) was added, and the samples were incubated at room temperature for 15 min. The labelled cells were washed three times with PBS and examined by using Olympus IX71 inverted fluorescence microscope. The images were captured by means of Cell F image acquiring system.

2.5. Cell viability and proliferation

The viability of EPCs on the surfaces was examined using the LIVE/DEAD Viability/Cytotoxicity Kit (Life Technologies, USA), as previously reported [27]. Briefly, the cells were seeded on the samples and, after incubation for various periods of time, they were stained for 10 min in PBS solution containing 2 μM calcein acetoxymethyl (AM) ester to label live cells and 4 μM ethidium homodimer-1 to label dead cells. An inverted fluorescent microscope (Olympus IX71) was used to record the fluorescent images after staining.

The proliferation of EPCs was monitored at 1- and 5- days post-seeding by performing the 3-(4,5-Dimethylthiazol-2-yl)-2,5-diphenyltetrazolium bromide (MTT) colorimetric assay. Briefly, the cell cultures were incubated with MTT solution (1 mg/ml in growth supplement free culture medium) for 3 h at 37 °C. Then, the MTT solution was decanted and formazan crystals were solubilized with dimethyl sulfoxide. Absorbance of the dye was measured at a wavelength of 550 nm and recorded using a microplate reader (Thermo Scientific Appliskan).

2.6. Endothelial cell markers analysis

The expression of vascular endothelial cell cadherin (VE-cadherin) and von Willebrand factor (vWf) within EPCs grown on the analyzed surfaces was examined as we previously described [28]. Briefly, after 5 days of in vitro growth, the culture media were removed and the cells were washed and fixed by immersion in 4% paraformaldehyde. After fixation, the EPCs were permeabilized by their incubation with 0.1% Triton-X100 in PBS for 15 min at room temperature. This treatment allowed the further access of the primary antibodies (monoclonal antibodies against VE-cadherin and vWf, respectively) to their epitopes. Alexa Fluor 488 and Alexa Fluor 546 conjugated secondary antibodies, respectively, were used for the microscopic visualization of the staining pattern. The cell nuclei were labelled with 4′6-diamidino-2- phenylindole (DAPI, blue).

2.7. Quantification of EPCs inflammatory response to the Ti–27Nb alloy

The inflammatory response of EPCs to the analyzed materials was evaluated by quantifying the protein levels of the MCP-1 secreted into cell culture media after 24 h of culture. These media were collected, centrifuged, and processed for MCP-1 measurement by using the specific sandwich enzyme-linked immunosorbent assay (ELISA) kit according to the manufacturer's instructions (R&D Systems) [29].

2.8. Statistical analysis

All quantitative data were expressed as means ± standard deviation (SD). One-way ANOVA with Bonferroni's multiple comparison test was used to assess the statistical significance of results between the analyzed groups. The P values lower than 0.05 were considered statistically significant.

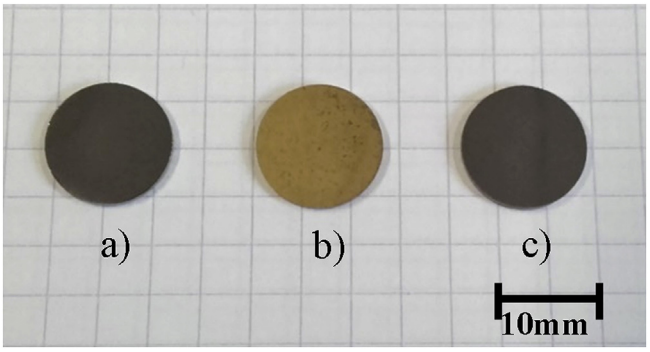

Fig. 1. Visual appearance of a) bare Ti–27Nb, nitrided Ti–27Nb, c) NiTi, alloy.

3. Results and discussions

3.1. Materials characterization

Fig. 1 shows the visual appearance of the samples. Metallic grey color is for the bare Ti–27Nb alloy (a) and the NiTi alloy (c), while a characteristic gold yellow color of titanium nitrides is observed on the Ti–27Nb alloy after the gas nitriding treatment (b).

The XRD patterns presented in Fig. 2 confirm the surface modification of Ti–27Nb alloy induced by the gas-nitriding treatment, and the detection of TiN and Ti_2N titanium nitrides in surface (Fig. 2).

Typical AFM maps obtained from each alloy are presented in Fig. 3. The uniform roughness can be observed from the Ti–27Nb samples before (a) and after gas nitriding treatment (b) and from NiTi (c).

Table 1 shows the roughness values, Ra, for each sample type evaluated from 10 scans. The Ra value of the Ti–27Nb sample increases to a value close to that of NiTi after the gas nitriding treatment.

3.2. Endothelial progenitor cell response

Cell adhesion on the surface of a material is one of the prerequisites for assessment of the material biological compatibility and its possible use in biomedical applications. The surface contact between cells and substrate is determinant for several factors such as cell morphology, cell proliferation and differentiation. In the current study, an investigation of the actin cytoskeleton organization (actin staining) and assembly of cell–matrix adhesions (vinculin staining) of EPCs has been conducted by immunofluorescence analysis to confirm the ability of Ti–27Nb material to sustain/enhance cell adhesion (Fig. 4). After 2 h of culture, EPCs in contact with the test materials exhibited well organized actin bundles and cell–matrix adhesions similar to those shown in cells

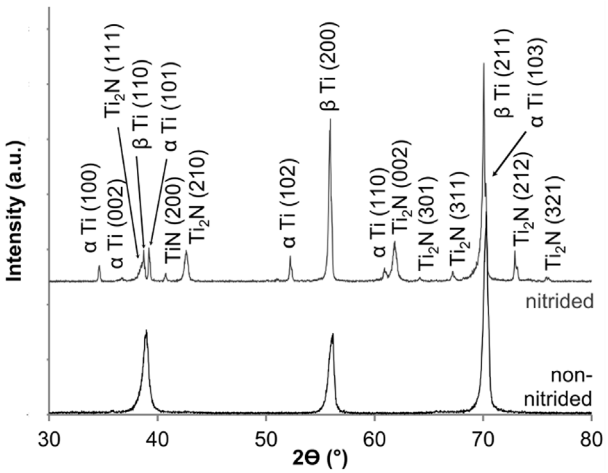

Fig. 2. XRD patterns of nitrided and non-nitrided Ti–27Nb alloy.

adhered to the reference biomaterial. This cellular behaviour could be explained by close surface roughness values in the nanometer range, as shown in Table 1. Morphologically, after 24 h in culture, the EPCs on all substrates exhibited the typical phenotype of endothelial cells (ECs).

Afterwards, the viability studies were carried out using Live/Dead kit assay. Live cells produce an intense uniform green fluorescence as they convert the non-fluorescent calcein AM to fluorescent calcein while ethidium homodimer-1 (EthD-1) enters the cells with damaged membranes producing a red fluorescence. This assay evinced an increase in the number of green stained cells on the fifth day of culture (Fig. 5a), allowing us to qualitatively evaluate the extension of cell proliferation. The cell proliferation was also assessed by MTT assay. The results shown in Fig. 5b indicate that the analyzed materials are able to support the cell proliferation along the culture period. The good agreement between the trend observed with the Live/Dead assay and MTT test confirms that the increased metabolic activity may be mainly attributed to an increased cell density. There are no differences in cell proliferation and metabolic activity over the test period of 5 days depending on the substrate. Therefore, all analyzed metallic samples do not exhibit any cytotoxicity and maintain exponential growth rates in short term culture.

Stent materials should not only induce good behaviour of EPCs in terms of cell spreading morphology, viability, attachment but also have to be appropriate to encourage EPCs' functions. Therefore, the protein expression of the functional markers of the endothelial cells, such as VE-cadherin and vWf were examined. The cell–cell junctional integrity of endothelial cells after material exposure was evaluated by epi-fluorescence using antibody against VE-cadherin. As seen in Fig. 6, VE-cadherin is found at the cell borders, outlining the cells in a regular pattern. Likewise, high resolution fluorescence images revealed a dotted pattern of vWf within the cytoplasm, mostly in the perinuclear region, in case of all samples. Taken together, these results indicate the preservation of endothelial cells' characteristic phenotype both on the bare and nitrided new alloy.

The prospective use of a biomaterial *in vivo* also depends on the absence of a significant pro-inflammatory activity associated with its presence. Endothelial cells play an important role in the regulation of immune and inflammatory local responses by expressing specific adhesion molecules and inflammatory cytokines such as interleukin (IL)-1, IL-8, and MCP-1, which in turn induce the selective recruitment of leukocytes to the areas of vascular interventions. Among these cytokines, the chemokine that is the predominant attractant for neutrophils is IL-8, while the predominant attractant for monocytes is MCP-1. It is acknowledged that neutrophils surrounding stent struts are only transiently present within days after stent implantation, while chronic inflammatory cells such as monocytes could be observed both in early (within 7 days) and late (6 months or later) stages after stenting [30]. *In vivo* studies [31] have shown that the chronic low-grade vascular inflammation aggravates restenosis; therefore the effective mitigation of the inflammatory response represents a well-recognized anti-restenosis strategy. In line with this, the studies conducted by Egashira et al. [32,33], aimed at developing a gene therapy strategy to inhibit the MCP-1 action by local delivery of a mutant MCP-1 protein, called 7ND, that functions as a dominant negative inhibitor of MCP-1. These studies demonstrated that the inhibition of MCP-1-mediated inflammation is effective in reducing in-stent restenosis after stent placement. Likewise, other studies support the notion that MCP-1 is a major player in the pathogenesis of the neointimal hyperplasia, and also provide evidence for the feasibility of therapeutic strategies targeting the reduction/inhibition of MCP-1 expression [34–36].

In the present study, the protein levels of secreted MCP-1 were quantified by ELISA technique and the results are shown in Fig. 7. There are no statistically significant differences occurred between the EPCs grown on the NiTi and bare Ti–27Nb alloy, despite important differences among their chemical composition. However, the surface nitriding treatment of Ti–27Nb material led to a significant decrease in

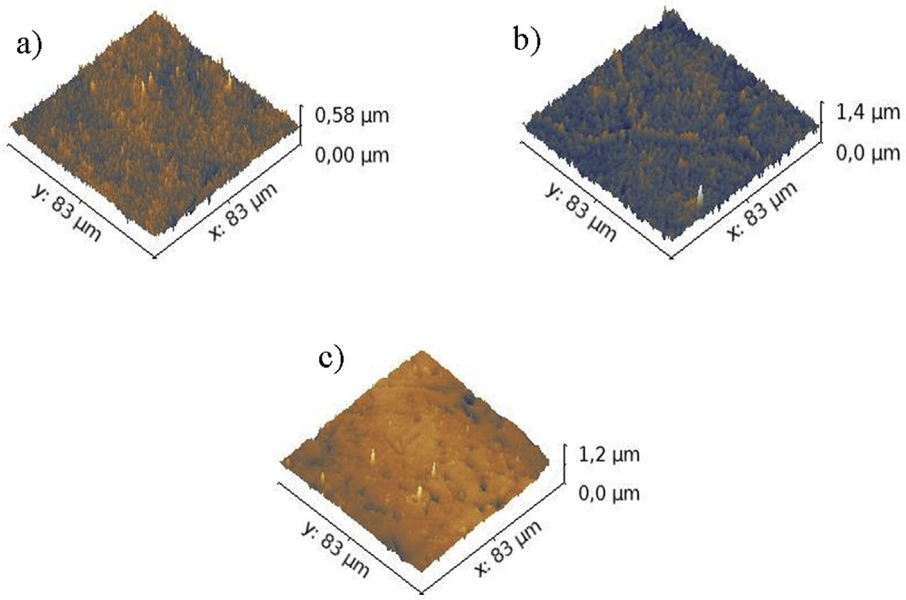

Fig. 3. AFM surface scans from: a) bare Ti–27Nb; b) nitrided Ti–27Nb; c) NiTi, alloy.

Table 1
Surface roughness, R_a values and standard deviation of the studied samples.

Sample	bare Ti–27Nb	nitrided Ti–27Nb	NiTi
Ra [nm]	21 ± 3	61 ± 6	53 ± 5

MCP-1 ($p < 0.05$) release. This finding suggests that the mitigation of the inflammatory EPC activation by the nitrided Ti–27Nb alloy characterized by significantly reduced MCP-1 expression is most likely due to protective effect of the nitride layer against metal corrosion and ion release.

In terms of clinical translation, reduced local expression of MCP-1 could control the influx and activation of macrophages during the distinct phases of the inflammatory response, leading to dampened inflammation throughout the foreign body response and resolution stages and thus limiting neointimal formation.

4. Conclusions

The interaction of a Ni-free Ti–27Nb alloy and its nitrided counterpart with EPCs has been investigated. The results showed that both analyzed materials support the attachment and spreading of EPCs. EPCs formed well-organized cell–matrix adhesions and fine-stretched actin bundles after 2 h of adhesion. Moreover, vinculin was prominently expressed during the adhesion of EPCs on test materials. The cellular survival and proliferation were expressed to a similar extent on all analyzed surfaces. In addition, immunofluorescence staining revealed that EPCs expressed tight junctions consisting of VE-cadherin and expressed vWf, suggesting the preservation of EPC phenotype. Surface nitriding treatment reduced the expression of the important pro-inflammatory and pro-atherogenic chemokine MCP-1 in EPCs, which indicates that this surface modification strategy holds promise in mitigating the local foreign body reaction (FBR) to stent biomaterials. These results contribute to a better understanding of EPCs interaction with titanium-based superelastic alloys and indicate that nitrided Ti–27Nb alloy should be further investigated as an alternative to the current metallic materials commonly used for stent implantation.

Acknowledgements

This study was financially supported by the Romanian Ministry of

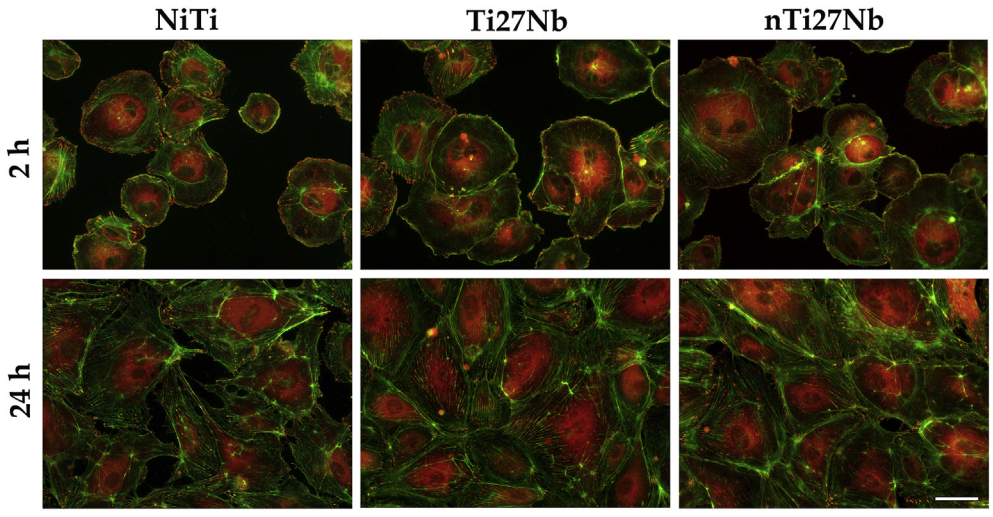

Fig. 4. Fluorescent microscopy images of EPC cells cultured for 2 h and 24 h on NiTi, bare Ti–27Nb and nitrided Ti–27Nb (nTi27Nb) surfaces. Actin microfilaments and vinculin are stained green and red. Scale bar represents 50 µm. (For interpretation of the references to color in this figure legend, the reader is referred to the Web version of this article.)

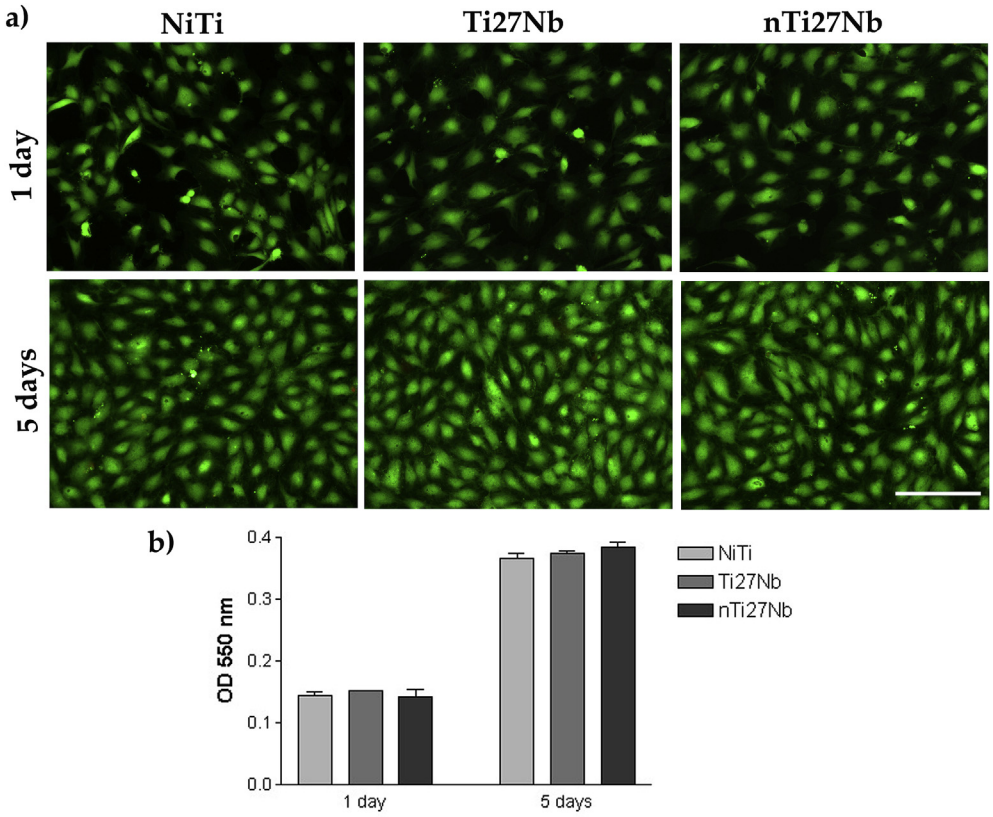

Fig. 5. (a) Viability and proliferation rate of EPCs grown on the analyzed surfaces for 1 day and 5 days, as assessed by Live & Dead assay (green = viable cells; red = dead cells); (b) MTT assay demonstrates a time-dependent increase in cell proliferation rate without significant differences between cells growing on the studied biomaterials at a certain time point. Scale bar represents 200 μm. (For interpretation of the references to color in this figure legend, the reader is referred to the Web version of this article.)

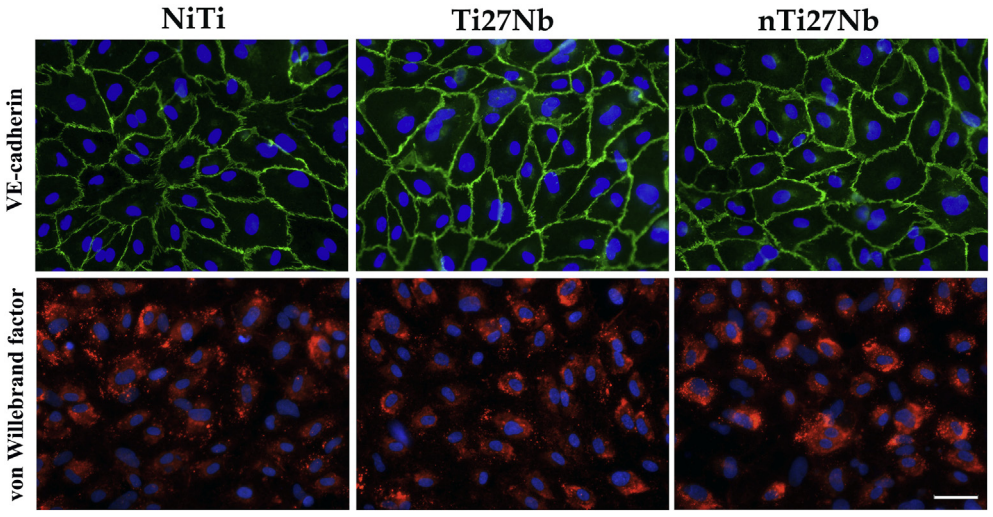

Fig. 6. Immunofluorescence detection of specific endothelial markers in EPCs grown in contact with the analyzed metallic samples for 5 days: VE-cadherin (green) and vWf (red). Nuclei (blue) were stained using DAPI. Scale bar = 50 μm. (For interpretation of the references to color in this figure legend, the reader is referred to the Web version of this article.)

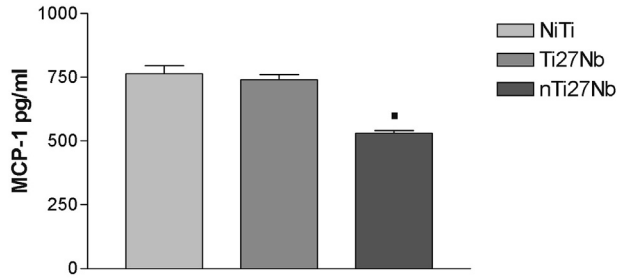

Fig. 7. Mean (± SD) levels of MCP-1 secreted into culture media after 24 h culture of EPCs on test samples, as detected by ELISA. ▪$p < 0.05$ *vs.* NiTi and Ti–27Nb.

National Education, CNCS-UEFISCDI (project PN-II-ID-20-RO-FR-2014).

Appendix A. Supplementary data

Supplementary data to this article can be found online at https://doi.org/10.1016/j.pnsc.2019.08.001.

References

[1] R. Koster, D. Vieluf, M. Kiehn, M. Sommerauer, J. Kahler, S. Baldus, T. Meinertz, C.W. Hamm, Lancet 356 (2000) 1895–1897 https://doi.org/10.1016/s0140-6736(00)03262-1.
[2] M. Goebeler, G. Meinardus-Hager, J. Roth, S. Goerdt, C. Sorg, J. Investig. Dermatol. 100 (1993) 759–765 https://doi.org/10.1111/1523-1747.ep12476328.
[3] D. Viemann, M. Schmidt, K. Tenbrock, S. Schmid, V. Muller, K. Klimmek, S. Ludwig,

J. Roth, M. Goebeler, J. Immunol. 178 (2007) 3198–3207 https://doi.org/10.4049/jimmunol.178.5.3198.
[4] E. McLucas, Y. Rochev, W.M. Carroll, T.J. Smith, J. Mater. Sci. Mater. Med. 19 (2008) 975–980 https://doi.org/10.1007/s10856-006-0087-9.
[5] M. Schmidt, B. Raghavan, V. Muller, T. Vogl, G. Fejer, S. Tchaptchet, S. Keck, C. Kalis, P.J. Nielsen, C. Galanos, J. Roth, A. Skerra, S.F. Martin, M.A. Freudenberg, M. Goebeler, Nat. Immunol. 11 (2010) 814–819 https://doi.org/10.1038/ni.1919.
[6] D. Yang, X. Lu, Y. Hong, T. Xi, D. Zhang, Biomaterials 35 (2014) 6195–6205 https://doi.org/10.1016/j.biomaterials.2014.04.069.
[7] M. Shayan, Y. Chun, Acta Biomater. 21 (2015) 20–34 https://doi.org/10.1016/j.actbio.2015.03.025.
[8] H.Y. Kim, Y. Ikehara, J.I. Kim, H. Hosoda, S. Miyazaki, Acta Mater. 54 (2006) 2419–2429 https://doi.org/10.1016/j.actamat.2006.01.019.
[9] M. Bonisch, M. Calin, J. van Humbeeck, W. Skrotzki, J. Eckert, Mater. Sci. Eng. C Mater. Biol. Appl. 48 (2015) 511–520 https://doi.org/10.1016/j.msec.2014.12.048.
[10] J. Fu, A. Yamamoto, H.Y. Kim, H. Hosoda, S. Miyazaki, Acta Biomater. 17 (2015) 56–67 https://doi.org/10.1016/j.actbio.2015.02.001.
[11] Y. Wang, Y. Zheng, Mater. Lett. 63 (2009) 1293–1295 https://doi.org/10.1016/j.matlet.2009.02.062.
[12] I. Jirka, M. Vandrovcova, O. Frank, Z. Tolde, J. Plšek, T. Luxbacher, L. Bačáková, V. Starý, Mater. Sci. Eng. C Mater. Biol. Appl. 33 (2013) 1636–1645 https://doi.org/10.1016/j.msec.2012.12.073.
[13] J. Xu, X.-J. Weng, X. Wang, J.-Z. Huang, C. Zhang, H. Muhammad, X. Ma, Q.-D. Liao, PLoS One 8 (2013) e79289https://doi.org/10.1371/journal.pone.0079289.
[14] R.E. McMahon, J. Ma, S.V. Verkhoturov, D. Munoz-Pinto, I. Karaman, F. Rubitschek, H.J. Maier, M.S. Hahn, Acta Biomater. 8 (2012) 2863–2870 https://doi.org/10.1016/j.actbio.2012.03.034.
[15] L. Shi, L. Wang, Y. Duan, W. Lei, Z. Wang, J. Li, X. Fan, X. Li, S. Li, Z. Guo, PLoS One 8 (2013) e55015https://doi.org/10.1371/journal.pone.0055015.
[16] D.P. de Andrade, L.M. de Vasconcellos, I.C. Carvalho, L.F. Forte, E.L. de Souza Santos, R.F. Prado, D.R. Santos, C.A. Cairo, Y.R. Carvalho, Mater. Sci. Eng. C Mater. Biol. Appl. 56 (2015) 538–544 https://doi.org/10.1016/j.msec.2015.07.026.
[17] L. Héraud, P. Castany, D. Lailllé, T. Gloriant, Mater. Today Proc. 2 (2015) S917–S920 https://doi.org/10.1016/j.matpr.2015.07.431.
[18] P. Castany, Y. Yang, E. Bertrand, T. Gloriant, Phys. Rev. Lett. 117 (2016) 245501 https://doi.org/10.1103/PhysRevLett.117.245501.
[19] Y. Bedouin, D.M. Gordin, P. Pellen-Mussi, F. Perez, S. Tricot-Doleux, C. Vasilescu, S.I. Drob, D. Chauvel-Lebret, T. Gloriant, J. Biomed. Mater. Res. B Appl. Biomater. 107 (5) (2018) 1483–1490 https://doi.org/10.1002/jbm.b.34240.
[20] V.-H. Pham, S.-H. Jun, H.-E. Kim, Y.-H. Koh, Appl. Surf. Sci. 258 (2012) 2864–2868 https://doi.org/10.1016/j.apsusc.2011.10.149.
[21] D.M. Gordin, T. Gloriant, V. Chane-Pane, D. Busardo, V. Mitran, D. Hoche, C. Vasilescu, S.I. Drob, A. Cimpean, J. Mater. Sci. Mater. Med. 23 (2012) 2953–2966 https://doi.org/10.1007/s10856-012-4750-z.
[22] D.M. Gordin, D. Busardo, A. Cimpean, C. Vasilescu, D. Hoche, S.I. Drob, V. Mitran, M. Cornen, T. Gloriant, Mater. Sci. Eng. C Mater. Biol. Appl. 33 (2013) 4173–4182 https://doi.org/10.1016/j.msec.2013.06.008.
[23] R. Ion, C. Vasilescu, P. Drob, E. Vasilescu, A. Cimpean, S.I. Drob, D.M. Gordin, T. Gloriant, Mater. Corros. 65 (2014) 593–604 https://doi.org/10.1002/maco.201206724.
[24] K.W. Yeung, R.W. Poon, P.K. Chu, C.Y. Chung, X.Y. Liu, W.W. Lu, D. Chan, S.C. Chan, K.D. Luk, K.M. Cheung, J. Biomed. Mater. Res. A 82 (2007) 403–414 https://doi.org/10.1002/jbm.a.31154.
[25] H. Li, B. Yuan, Y. Gao, C.Y. Chung, M. Zhu, J. Biomed. Mater. Res. A 99 (2011) 544–553 https://doi.org/10.1002/jbm.a.33198.
[26] R. Ion, C. Luculescu, A. Cimpean, P. Marx, D.M. Gordin, T. Gloriant, Mater. Sci. Eng. C Mater. Biol. Appl. 62 (2016) 686–691 https://doi.org/10.1016/j.msec.2016.02.031.
[27] V. Mitran, M.G. Albu, E. Vasile, A. Cimpean, M. Costache, Prog. Nat. Sci. Mater. Int. 25 (2015) 122–130 https://doi.org/10.1016/j.pnsc.2015.03.008.
[28] R. Ion, S.I. Drob, M.F. Ijaz, C. Vasilescu, P. Osiceanu, D.M. Gordin, A. Cimpean, T. Gloriant, Materials 9 (2017), https://doi.org/10.3390/ma9100818.
[29] P. Neacsu, D.M. Gordin, V. Mitran, T. Gloriant, M. Costache, A. Cimpean, Mater. Sci. Eng. C Mater. Biol. Appl. 47 (2014) 105–113 https://doi.org/10.1016/j.msec.2014.11.023.
[30] T. Inoue, K. Croce, T. Morooka, M. Sakuma, K. Node, D.I. Simon, Interv 4 (2011) 1057–1066 https://doi.org/10.1016/j.jcin.2011.05.025.
[31] A. Farb, D.K. Weber, F.D. Kolodgie, A.P. Burke, R. Virmani, Circulation 105 (2002) 2974–2980 https://doi.org/10.1161/01.CIR.0000019071.72887.BD.
[32] K. Ohtani, M. Usui, K. Nakano, Y. Kohjimoto, S. Kitajima, Y. Hirouchi, X.-H. Li, S. Kitamoto, A. Takeshita, K. Egashira, Gene Ther. 11 (2004) 1273–1282 https://doi.org/10.1038/sj.gt.3302288.
[33] K. Egashira, K. Nakano, K. Ohtani, K. Funakoshi, G. Zhao, Y. Ihara, J. Koga, S. Kimura, R. Tominaga, K. Sunagawa, Arterioscler. Thromb. Vasc. Biol. 27 (2007) 2563–2568 https://doi.org/10.1161/ATVBAHA.107.154609.
[34] K. Egashira, M. Koyanagi, S. Kitamoto, W. Ni, C. Kataoka, R. Morishita, Y. Kaneda, C. Akiyama, K. Nishida, K. Sueishi, A. Takeshita, FASEB J. 14 (2000) 1974–1978 https://doi.org/10.1096/fj.00-0141com.
[35] K. Egashira, Q. Zhao, C. Kataoka, K. Ohtani, M. Usui, I.F. Charo, K. Nishida, S. Inoue, M. Katoh, T. Ichiki, A. Takeshita, Circ. Res. 90 (2002) 1167–1172.
[36] M. Usui, K. Egashira, K. Ohtani, C. Kataoka, M. Ishibashi, K. Hiasa K, M. Katoh, Q. Zhao, S. Kitamoto, A. Takeshita, FASEB J. 16 (2002) 1838–1840 https://doi.org/10.1096/fj.02-0094fje.